JOURNAL OF MATERIALS SCIENCE 26 (1991) 5585–5594

Dissolution slowness surfaces of cubic crystals

Part 1 *Theory and three-dimensional representation for class 23*

A. BRAHIM-BOUNAB, J. Y. AMAUDRUT, C. R. TELLIER
Laboratoire de Chronométrie, Electronique et Piézoélectricité, Ecole Nationale Superieure de Mecanique et des Microtechniques, Route de Gray, La Bouloie, 25030 Besançon Cedex, France

The first part of this paper offers a tensorial method that gives analytical equations for the dissolution slowness surface of cubic crystals. Conditions for the proposed equations are outlined. The non-centrosymmetric class 23 is treated as an example. The evolution of the shape of the slowness surface with the higher rank of the dissolution tensors is studied, using in particular a three-dimensional graphical representation of the slowness surface. The conditions for obtaining slowness surfaces with a complex shape and an increasing number of extrema are discussed.

1. Introduction

The anisotropic etching of semiconductor crystals such as silicon [1–5], germanium [1, 5–8] and gallium arsenide [1, 9–11] is a widely used process in microelectronic device fabrication [1, 2] which has been used in particular to obtain V – groove structures [9, 12, 13] in silicon and gallium arsenide wafers. Moreover, in the past few years several attempts [2, 11, 14–25] have been made to apply the photolithographic process to the micromachining of mechanical devices, which constitute the sensing element of silicon integrated sensors. The fabrication techniques in the field of micromechanical devices are always based on anisotropic etching processes [2, 11]. The bias-controlled doping-selective etching technology [2, 26–28] appears only as a complementary process which is used for the possibility it offers of controlling the geometry of particular micromachined mechanical structures, such as cantilever beams [26–28]. It should be noted that the mechanical performance of micromachined devices depends on their geometry. For example, when using potassium–water and EPW (ethylenediamine–pyrocathecol–water) solutions for the anisotropic etching of (1 0 0)-oriented silicon wafers, the main difficulty arises from the corner undercutting [3, 4, 29–31]. Some methods have recently been proposed to reduce corner undercutting [4, 30, 31], the most efficient method involving a mask-compensation technique [31].

Most silicon-integrated sensors are piezoresistive sensors [14, 15, 21–24, 32–37] which have been developed to measure forces, pressures, displacements and accelerations. Many silicon sensors consist of four semiconductor strain gauges in the form of a Wheatstone bridge [22–24, 36, 37]. But recently new structures have been studied, such as pressure sensors composed of a single element with four terminals arranged like a Hall element [15, 32–35]. Designs of strain gauges as well as four terminal sensors require the determination of particular orientations, for which the sensitivity and the resolution of sensors must become optimum [15, 32, 34, 37, 38]. The optimization of sensor geometry can involve the etching of micromechanical devices in wafers whose orientations differ from those commonly used in the semiconductor industry (e.g. the (1 0 0) (1 1 0) and (1 1 1) silicon-oriented wafers).

If the fabrication process starts with differently oriented wafers, we need to deal with a three-dimensional theoretical model for anisotropic etching which offers the possibility of predicting easily the exact geometrical features of etched micromechanical devices. Tellier and co-workers have recently suggested that this be done using a tensorial analysis of dissolution [39–42] provided the etching process can be described by kinematic theory [1, 43–46]. Part I of this paper applies tensorial analysis to the anisotropic etching of crystals belonging to the cubic system, in order to derive generalized equations for the representative surface of the dissolution slowness vector, **L**, [39, 47] in the case of centrosymmetric (m3, 432, m3m) and non-centrosymmetric (23, $\bar{4}$3m) classes. Emphasis is placed on the necessity of developing calculations to tensors of higher ranks when marked anisotropy in etching is observed. The case of class 23 is treated as an example. For a full exploitation of the tensorial method, application in the fields of theoretical and graphical simulation of etched shapes and of the design of micromachined mechanical structures are presented in part II [51]. Methods to predict the shapes of sections for etched grooves and to evaluate the extent of the under-etching are proposed. The slowness surfaces and some polar graphs of the dissolution slowness related to class 23 are used to illustrate these possibilities.

0022–2461/91 $03.00 + .12

2. Theory

2.1. Expressing the dissolution slowness surface

In practice, the surface of a crystal of more and less complex geometrical shape can always be decomposed in a great number of planar surface elements whose orientations correspond to those related to given crystallographic planes. When the dissolution process of a crystal is anisotropic, the various surface elements move within the crystal along different trajectories. We can represent the displacement of a given moving surface element by a propagation vector, **P**, [39, 43, 47] whose magnitude and direction depends on the orientation of the surface element. Tellier and co-workers [39, 43, 47] have recently shown that the propagation vectors associated with the various planar surface elements can be completely determined starting from the equation expressing the representative surface of the dissolution slowness vector, **L**, the so-called slowness surface.

The simplest way to derive the equation for the slowness surface is to express the magnitude, L, of the slowness vector **L** in terms of a polynomial regression involving the three Cartesian components (n_1, n_2, n_3) of the unit inward normal **n** to a surface element [39, 40, 47]. Effectively, as the components n_1, n_2 and n_3 vary, the orientation (φ, θ) of the surface element is changed causing the displacement of the extremity of **L** along the slowness surface. Then L may be written in the compact form

$$L = D_0 + D_i n_i + D_{ij} n_i n_j + D_{ijk} n_i n_j n_k + D_{ijkl} n_i n_j n_k n_l + \ldots \quad (1)$$

where the coefficients D_0, D_i, D_{ij}, D_{ijk}, D_{ijkl}, denote the components of dissolution tensors with increasing rank N.

From the definition of L, it follows that all the subscripts can be interchanged [39]. This constitutes a first procedure to reduce the number of dissolution constants. In a second step we have to consider the symmetry of point groups to identify the independent dissolution constants and completely to characterize the dissolution process for the cubic crystal system. Because some symmetry point groups are centrosymmetric, we need to follow this procedure for tensors up to rank 10.

2.2. Dissolution constants for class 23

In this section we deal with the minimum symmetry point group 23. Then we have only to consider the following properties [48].

1. Class 23 has three two-fold rotation axes which are chosen parallel to the Cartesian reference axes (x_1, x_2, x_3).
2. The four three-fold rotation axes along the cube diagonals cyclically permute the subscripts.

Let us firstly consider a transformation from axes (x_1, x_2, x_3) to primed axes (x'_1, x'_2, x'_3) in which the dissolution constants are changed in primed dissolution constants, and secondly, deal with the symmetry transformations associated with point group 23. Taking successively the operator 2 along the axes x_1, x_2 and x_3 gives respectively

$$x'_1 = x_1, x'_2 = -x_2, x'_3 = -x_3 \quad (2)$$

$$x'_1 = -x_1, x'_2 = x_2, x'_3 = -x_3 \quad (3)$$

$$x'_1 = -x_1, x'_2 = -x_2, x'_3 = x_3 \quad (4)$$

Then we have just to recall that the dissolution constants transform, as do the product of corresponding coordinates [49] and that the symmetry operation 2 along x_1, x_2 and x_3 must leave the dissolution constants unchanged to obtain the constants which do not vanish.

To illustrate this procedure, we can for example consider some constants appearing in tensors of ranks 7 and 8. According to Equation 2 we have

$$D'_{1122222} = D_{1122222} \rightarrow -D_{1122222} \text{ since } x_1^2 x_2^5 \rightarrow -x_1^2 x_2^5$$

$$D'_{12222222} = D_{12222222} \rightarrow -D_{12222222} \text{ since } x_1 x_2^7 \rightarrow -x_1 x_2^7 \quad (5)$$

From relation 5, we infer that the dissolution constants involving only one or two different subscripts vanish when the number of one of the subscripts is odd. In other words, the remaining dissolution constants are those with a combination of an even number of subscripts 1 and/or 2 and/or 3, or with an odd number of the three subscripts.

Applying this condition to the sensor of rank 7 gives the dissolution constants which do not vanish

$$D_{3333312}, D_{1111123}, D_{2222213}, D_{1112333}, D_{1112223}, D_{2223331} \quad (6)$$

Further permuting the subscripts 1, 2 and 3 cyclically leads to the complementary relations

$$D_{1111123} = D_{2222213} = D_{3333312} \quad (7)$$

$$D_{1112223} = D_{1113332} = D_{2223331} \quad (8)$$

so that the number of independent dissolution constants reduces to two.

It is also of interest to mention that by applying the symmetry transformations related to point group 23 to tensors of ranks 6, 8 and 10, we distinguish two kinds of relations for the dissolution constants having unequal even numbers of two subscripts ij (e.g. of respective forms D_{iijjjj}, $D_{iijjjjjj}$, $D_{iijjjjjjjj}$ and $D_{iiiijjjjjj}$). For the tensor of rank 10, the double symmetry relations are expressed as

$$D_{1122222222} = D_{3311111111} = D_{2233333333}$$

$$D_{1133333333} = D_{2211111111} = D_{3322222222} \quad (9)$$

$$D_{1111222222} = D_{3333111111} = D_{2222333333}$$

$$D_{1111333333} = D_{2222111111} = D_{3333222222} \quad (10)$$

From these considerations, Table I lists the non-vanishing dissolution constants for tensors of ranks up to 10. We observe that the number of independent constants for tensors of odd rank increases from one for $N = 1$ to four for $N = 9$. For tensors of even rank,

TABLE I Relations between dissolution constants for class 23. A, B, C, D, E refer to double relations

Rank N_{max}	Relations between dissolution constants		n_N
0	D_0		1
1	All the constants vanish		0
2	$D_{11} = D_{22} = D_{33}$		1
3	D_{123}		1
4	$D_{1111} = D_{2222} = D_{3333}$; $D_{1122} = D_{1133} = D_{2233}$		2
5	$D_{11123} = D_{22213} = D_{33312}$		1
6	$D_{111111} = D_{222222} = D_{333333}$; D_{112233}		4
	$D_{111122} = D_{113333} = D_{222233}$; $D_{111133} = D_{112222} = D_{223333}$	A	
7	$D_{1111123} = D_{1222223} = D_{1233333}$; $D_{1112223} = D_{1222333} = D_{1112333}$		2
8	$D_{11111111} = D_{22222222} = D_{33333333}$ $D_{11112222} = D_{11113333} = D_{22223333}$ $D_{11112233} = D_{11222233} = D_{11223333}$ $D_{11111122} = D_{22222233} = D_{11333333}$; $D_{11111133} = D_{11222222} = D_{22333333}$	B	5
9	$D_{111222333}$; $D_{111111123} = D_{122222223} = D_{123333333}$		4
	$D_{111112223} = D_{122222333} = D_{111233333}$; $D_{111112333} = D_{111222223} = D_{122233333}$	C	
10	$D_{1111111111} = D_{2222222222} = D_{3333333333}$		7
	$D_{1111112233} = D_{1122222233} = D_{1122333333}$; $D_{1111222233} = D_{1122223333} = D_{1111223333}$		
	$D_{1111111122} = D_{2222222233} = D_{1133333333}$; $D_{1111111133} = D_{1122222222} = D_{2233333333}$	D	
	$D_{1111112222} = D_{2222223333} = D_{1111333333}$; $D_{1111113333} = D_{1111222222} = D_{2222333333}$	E	

TABLE II Dissolution constants which must vanish when we pass from class 23 to class m3

$D_{123} = 0$, $D_{11123} = 0$, $D_{1111123} = 0$, $D_{1112223} = 0$, $D_{111112223} = 0$, $D_{111112333} = 0$

according to Table I, we have only one fundamental dissolution constant for the zero-rank tensor and seven fundamental dissolution constants referred to crystallographic axes for the tenth-rank tensor.

2.3. Dissolution constants for other cubic classes

The class m3 which has also three equivalent twofold rotation axes shows a higher degree of symmetry than the class 23 because it possesses a centre of symmetry. To pass from class 23 to class m3 it is only necessary to take the dissolution constants for tensors of odd ranks as zero (Table II).

On the other hand, for the non-centrosymmetric class $\bar{4}3m$ we have to retain the independent dissolution constants corresponding to tensor of odd rank. However it must be kept in mind that the class $\bar{4}3m$ possesses three four-fold rotation–inversion axes lying parallel to the reference Cartesian axes. For the transformations where the $\bar{4}$ axis coincides successively with the x_1, x_2 and x_3 axes, coordinates x_i' in the new-rotated system are expressed in terms of the unprimed coordinates by means of the following equations [41]:

$$x_1' = -x_1, x_2' = -x_3, x_3' = x_2 \quad (11)$$

$$x_1' = x_3, x_2' = -x_2, x_3' = -x_1 \quad (12)$$

$$x_1' = -x_2, x_2' = x_1, x_3' = -x_3 \quad (13)$$

The dissolution constants in Table I are divided into two groups of relations. Taking the $\bar{4}$ axis along the x_1 axis, it readily appears that relation 11 leads to

$$D'_{111112333} \rightarrow D_{111113222} \quad \text{since} \quad x_1'^5 x_2' x_3'^3 \rightarrow x_1^5 x_3 x_2^3 \quad (14)$$

conversely we have

$$D'_{111113222} \rightarrow D_{111112333} \quad \text{since} \quad x_1'^5 x_3' x_2'^3 \rightarrow x_1^5 x_2 x_3^3 \quad (15)$$

Then accounting for the fact that the double relations (A), (B), (C), (D) and (E) in Table I are replaced by single relations, the number of independent constants are finally affected, as indicated in Table III.

The classes 432 and m3m differ from class 23 in that three four-fold rotation axes replace the preceding three two-fold rotation axes, plus the fact that the classes 432 and m3m are centrosymmetric [48]. Then the specific relations associated with the three

TABLE III Additional relations between fundamental dissolution constants when we pass from class 23 to class $\bar{4}3m$. n_N is the number of independent dissolution constant for a tensor of rank N. One may note that for tensors of even rank the relations between the dissolution constants are identical to those listed in Table IV.

Rank N_{max}	Additional relations	n_N
6	$D_{111122} = D_{111133}$	3
8	$D_{11111122} = D_{11111133}$	4
9	$D_{111112223} = D_{111112333}$	3
10	$D_{1111111122} = D_{1111111133}$ $D_{1111112222} = D_{1111113333}$	5

operator 4 become

$$x_1' = x_1, x_2' = x_3, x_3' = -x_2 \quad (16)$$

$$x_1' = -x_3, x_2' = x_2, x_3' = x_1 \quad (17)$$

$$x_1' = x_2, x_2' = -x_1, x_3' = x_3 \quad (18)$$

according to which one may assert that the remaining dissolution constants are those with an even number of subscripts 1 and/or 2, and/or 3 which belong to tensors of even rank (Table III). According to Table III, the equations relating the dissolution constants of the form D_{iijjjj} or $D_{iijjjjjj}$ or $D_{iijjjjjjjj}$ or $D_{iiiijjjjjj}$ with $i \neq j$ are again not decoupled [41].

2.4. The generalized equation for the slowness surface of class 23

The general procedure for determining the generalized equation of a slowness surface is firstly to express the compact Equation 1 as a series in powers of the cartesian components of **n**. For the unit inward normal **n** we have

$$n_1^2 + n_2^2 + n_3^2 = 1 \quad (19)$$

If we substitute Equation 19 into the expanded equation for L and retain only terms related to the non-vanishing dissolution constants, it is now a simple matter to show that

$$\begin{aligned} L(n_1, n_2, n_3) = {} & D_0 + D_{11} + 6D_{123}n_1n_2n_3 + D_{1111}(n_1^4 + n_2^4 + n_3^4) + 6D_{1122}(n_1^2n_2^2 + n_1^2n_3^2 + n_2^2n_3^2) \\ & + 20D_{11123}n_1n_2n_3 + D_{111111}(n_1^6 + n_2^6 + n_3^6) + 15D_{111122}(n_1^4n_2^2 + n_2^4n_3^2 + n_3^4n_1^2) \\ & + 15D_{111133}(n_1^4n_3^2 + n_2^4n_1^2 + n_3^4n_2^2) + 90D_{112233}n_1^2n_2^2n_3^2 + 42D_{1111123}n_1n_2n_3(n_1^4 + n_2^4 \\ & + n_3^4) + 140D_{1112223}n_1n_2n_3(n_1^2n_2^2 + n_1^2n_3^2 + n_2^2n_3^2) + D_{11111111}(n_1^8 + n_2^8 + n_3^8) \\ & + 28D_{11111122}(n_1^6n_2^2 + n_2^6n_3^2 + n_3^6n_1^2) + 28D_{11111133}(n_1^6n_3^2 + n_2^6n_1^2 + n_3^6n_2^2) \\ & + 70D_{11112222}(n_1^4n_2^4 + n_1^4n_3^4 + n_2^4n_3^4) + 420D_{11112233}n_1^2n_2^2n_3^2 + 72D_{111111123} \\ & \times n_1n_2n_3(n_1^6 + n_2^6 + n_3^6) + 504D_{111112223}n_1n_2n_3(n_1^4n_2^2 + n_2^4n_3^2 + n_3^4n_1^2) \\ & + 504D_{111112333}n_1n_2n_3(n_1^4n_3^2 + n_2^4n_1^2 + n_3^4n_2^2) + 1680D_{111222333}n_1^3n_2^3n_3^3 \\ & + D_{1111111111}(n_1^{10} + n_2^{10} + n_3^{10}) + 45D_{1111111122}(n_1^8n_2^2 + n_2^8n_3^2 + n_3^8n_1^2) \\ & + 45D_{1111111133}(n_1^8n_3^2 + n_2^8n_1^2 + n_3^8n_2^2) + 210D_{1111112222}(n_1^6n_2^4 + n_2^6n_3^4 \\ & + n_3^6n_1^4) + 210D_{1111113333}(n_1^6n_3^4 + n_2^6n_1^4 + n_3^6n_2^4) + 1260D_{1111112233}n_1^2n_2^2n_3^2(n_1^4 + n_2^4 \\ & + n_3^4) + 3150D_{1111222233}n_1^2n_2^2n_3^2(n_1^2n_2^2 + n_1^2n_3^2 + n_2^2n_3^2) \end{aligned} \quad (20)$$

In the second step we have to specify the successive rotations about coordinate axes which are needed to reach the final orientation of an arbitrary crystal plate. If we adopt the specifications proposed in the IEEE standard on piezoelectricity [48], the rotation angles φ and θ are those indicated in Fig. 1: the first rotation of amount φ is about the x_3 axis and the second rotation of amount θ about the x_1 axis. Then a doubly rotated surface element whose orientation is designated by (φ, θ) has a unit inward normal **n** whose Cartesian components in the reference system (x_1, x_2, x_3) are given by

$$n_1 = \sin\varphi\cos\theta, \quad n_2 = -\cos\varphi\cos\theta, \quad n_3 = -\sin\theta \quad (21)$$

If we substitute Equation 21 into Equation 20, simple but tedious calculations yield the generalized equation of the slowness surface in the form

$$L(\varphi, \theta) = S_1 + S_2 + S_3 + \mathscr{S}_1 + \mathscr{S}_2 + \mathscr{S}_3 \quad (22)$$

with

$$S_1 = \sum_{k=0} a_k \cos^{2k}\theta \sin^{2k}\theta \quad (23)$$

$$S_2 = \sum_{l=1} \sum_{m=0} b_{l,m} (\sin\varphi\cos\varphi\cos^2\theta)^{2l} (\cos\theta)^{2m} \quad (24)$$

$$S_3 = \sum_{L=0} \sum_{M=0} \mathscr{C}_{L,M} (\cos\varphi\cos\theta)^{2L} (\cos\theta)^{2M} \quad (25)$$

$$\mathscr{S}_l = \sum_{r=0} c_r (\sin 2\varphi \sin 2\theta \cos\theta)^{2r+l} \quad (26)$$

$$\mathscr{S}_2 = \sum_{s=0} \sum_{t=0} d_{s,t} \sin\theta (\sin\varphi\cos\varphi\cos^2\theta)^{2s+l} (\cos\theta)^{2t} \quad (27)$$

$$\mathscr{S}_3 = \sum_{P=0} \sum_{Q=0} \sum_{R=0} \mathscr{D}_{P,Q,R} (\sin\varphi\cos\varphi\sin\theta\cos^2\theta)^{2P+l} \times (\cos\varphi\cos\theta)^{2Q} (\cos\theta)^{2R} \quad (28)$$

Thus the series S_1, S_2 and S_3 are associated with tensors of even rank, whereas the series $\mathscr{S}_1$, $\mathscr{S}_2$ and $\mathscr{S}_3$ come from tensors of odd rank. Moreover, the coefficients $\mathscr{D}_{P,Q,R}$ with $P = 1$ involved in the series $\mathscr{S}_3$ are expressed in terms of dissolution constants which belong to tensors whose rank N is higher than 13. Then in most cases it can be shown easily that an appropriate relation for $\mathscr{S}_3$ may be

$$\mathscr{S}_3 = \sum_{Q=0} \sum_{R=0} \mathscr{D}_{Q,R} \sin\varphi\cos\varphi\sin\theta\cos^2\theta \times (\cos\varphi\cos\theta)^{2Q} (\cos\theta)^{2R}; \; N_{\max} < 13 \quad (29)$$

where $N_{\max}$ denotes the higher rank of tensors.

At this point it may be of interest to remark that an adequate use of the generalized Equation 22 requires some caution. Firstly, let us recall that the coefficients appearing in the six series are expressed in terms of the independent dissolution constants. Then it readily appears that to reflect the symmetry of the class 23, these

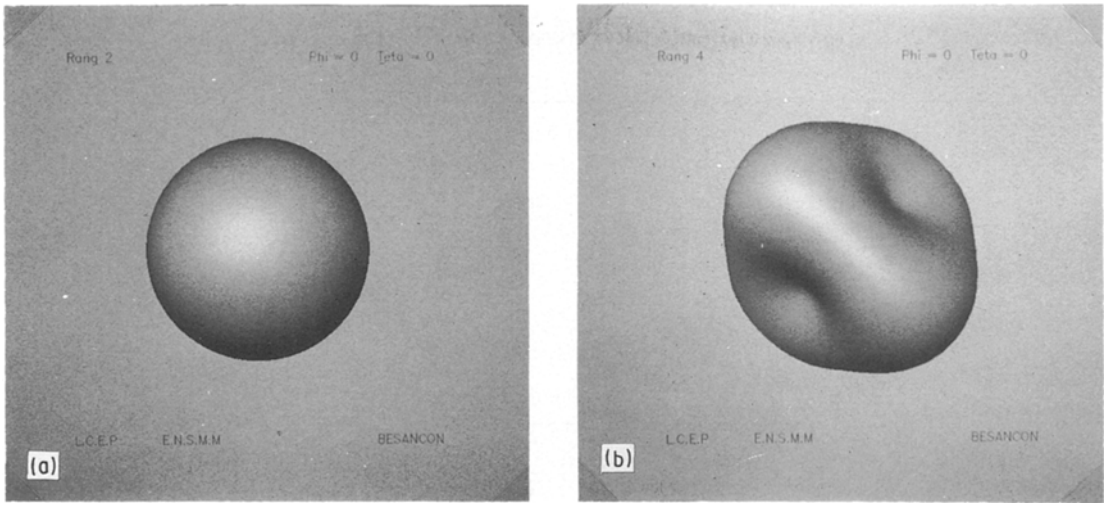

Figure 1 Slowness surface (a) Rang 2; (b) Rang 4

coefficients must satisfy the following conditions imposed by the crystal symmetry:

$$\mathscr{C}_{0,0} = 0; \quad b_{0,0} = 0; \quad \mathscr{D}_{0,0} = 0 \tag{30}$$

$$\sum_m b_{l,m} = a_l \tag{31}$$

$$\sum_M \mathscr{C}_{0,M} = 0 \tag{32}$$

$$\sum_R \mathscr{D}_{0,R} = 0 \tag{33}$$

$$\sum_M \mathscr{C}_{2,M} + \sum_M \mathscr{C}_{3,M} + \sum_M \mathscr{C}_{4,M} + \sum_M \mathscr{C}_{5,M} = -\sum_M \mathscr{C}_{1,M}; \quad N_{\max} = 10 \tag{34}$$

$$\sum_R \mathscr{D}_{2,R} + \sum_R \mathscr{D}_{3,R} = -\sum_R \mathscr{D}_{1,R}; \quad N_{\max} = 10 \tag{35}$$

Secondly, one may see that as the rank $N_{\max}$ increases, Equation 22 contains more and more coefficients. However, care must be taken that the order in which these additional coefficients are to be taken into account is by no means fortuitous. In reality it is possible to specify the number of coefficients involved in the general equation of the slowness surface by means of symmetry rules summarized in Table V which gives all the possible values for the summation indexes with respect to $N_{\max}$. Applying these selection rules in the special case where $N_{\max} = 7$ leads, for example, to

$$\begin{aligned} L(\varphi,\theta)_{N_{\max}=7} = L_7 = {} & a_0 + a_1(\cos\theta\sin\theta)^2 \\ & + (\sin\varphi\cos\varphi\cos^2\theta)^2[b_{1,0} + b_{1,1}\cos^2\theta] \\ & + (c_0 + d_{0,0}/4)\sin 2\varphi\cos 2\theta\cos\theta + \mathscr{C}_{0,1}\cos^2\theta \\ & + \mathscr{C}_{0,2}\cos^4\theta + \mathscr{C}_{0,3}\cos^6\theta + (\cos\varphi\cos\theta)^2 \\ & \times [\mathscr{C}_{1,0} + \mathscr{C}_{1,1}\cos^2\theta + \mathscr{C}_{1,2}\cos^4\theta] \\ & + (\cos\varphi\cos\theta)^4[\mathscr{C}_{2,0} + \mathscr{C}_{2,1}\cos^2\theta] \\ & + \mathscr{C}_{3,0}(\cos\varphi\cos\theta)^6 + \sin\theta(\sin\varphi\cos\varphi\cos^2\theta) \\ & \times [d_{0,1}\cos^2\theta + d_{0,2}\cos^4\theta] \\ & + d_{1,0}\sin\theta(\sin\varphi\cos\varphi\cos^2\theta)^3 \end{aligned} \tag{36}$$

Finally, we call attention to the fact that the compact expression (Equation 25) for the series S_3 has been obtained after some mathematical manipulations. Effectively the series S_3 is connected to double rotations

TABLE IV Identification of the independent dissolution constants for classes 4 3 2 and m 3 m

Rank $N_{\max}$	Relations between dissolution constants and independent constants	n_N
0	D_0	1
2	$D_{11} = D_{22} = D_{33}$	1
4	$D_{1111} = D_{2222} = D_{3333}$ $D_{1122} = D_{1133} = D_{2233}$	2
6	$D_{111111} = D_{222222} = D_{333333}$ $D_{111122} = D_{111133} = D_{112222} = D_{113333} = D_{222233} = D_{223333}$ D_{112233}	3
8	$D_{11111111} = D_{22222222} = D_{33333333}$ $D_{11111122} = D_{11111133} = D_{11222222} = D_{11333333} = D_{22222233} = D_{22333333}$ $D_{11112222} = D_{11113333} = D_{22223333}$ $D_{11112233} = D_{11222233} = D_{11223333}$	4
10	$D_{1111111111} = D_{2222222222} = D_{3333333333}$ $D_{1111111122} = D_{1111111133} = D_{1122222222} = D_{1133333333} = D_{2222222233} = D_{2233333333}$ $D_{1111112222} = D_{1111113333} = D_{1111222222} = D_{1111333333} = D_{2222223333} = D_{2222333333}$ $D_{1111112233} = D_{1122222233} = D_{1122333333}$ $D_{1111222233} = D_{1111223333} = D_{1122223333}$	5

TABLE V Selection rules for coefficients appearing in Equation 22 when the rank N_{max} varies from 0 to 10

Coefficients	Selection rules
a_k	$4k \leqslant N_{max}$ if N_{max} is even, $4k < N_{max}$ if N_{max} is odd
$b_{l,m}$	$4l + 2m \leqslant N_{max}$ if N_{max} is even; $4l + 2m < N_{max}$ if N_{max} is odd
$\mathscr{C}_{L,M}$	$2L + 2M \leqslant N_{max}$ if N_{max} is even; $2L + 2M < N_{max}$ if N_{max} is odd; $N_{max} \geqslant 6$
c_r	$N_{max} = 3(2r + 1)$ with N_{max} odd
$d_{s,t}$ $d_{0,t}$	$2t < N_{max} - 3$ if t is odd and $N_{max} \geqslant 5$ $2t \leqslant N_{max} - 3$ if t is even and $N_{max} \geqslant 5$
$d_{s,t}$ $d_{1,t}$	$2t < N_{max} - 6$ if t is odd and $N_{max} \geqslant 7$ $2t \leqslant N_{max} - 6$ if t is even and $N_{max} \geqslant 7$
$\mathscr{D}_{Q,R}$	$2Q + R \leqslant N_{max} - 3$ if N_{max} is odd; $2Q + R < N_{max}$ if N_{max} is even and $N_{max} \geqslant 9$

between the dissolution constants for tensors of rank $N \geq 6$. Then combining Equations 20 and 21 leads to the alternative expression for S_3.

$$S_3 = \sum_{L=1}\sum_{M=1} (\sin\varphi\cos\varphi\cos^2\theta)^{2L}[A_{L,M}(\sin\varphi\cos\theta)^{2M} + B_{L,M}(\cos\varphi\cos\theta)^{2M}] + (\sin\varphi\cos\theta\sin\theta)^{2L} \times [A_{L,M}(\sin\theta)^{2M} + B_{L,M}(\sin\varphi\cos\theta)^{2M}] + (\cos\varphi\cos\theta\sin\theta)^{2L}[A_{L,M}(\cos\varphi\cos\theta)^{2M} + B_{L,M}(\sin\theta)^{2M}] \quad (37)$$

We see immediately that if one transforms terms of the form $(\sin\gamma)^{2K}$ into sums in ascending powers of $\cos\gamma$, we are now in a position to show that Equation 37 reduces to Equation 25. A similar procedure has been followed to obtain the series $\mathscr{S}_3$ in the condensed forms 28 and 29 which contain ascending powers of $(\cos\varphi\cos\theta)^{2Q}$ and of $(\cos\theta)^{2R}$.

2.5. Generalized equations for the slowness surface of other cubic classes

For the class m 3 the simultaneous examinations of Table II and Equation 22 give L as

$$L = S_1 + S_2 + S_3 \quad (38)$$

In this equation the expressions for S_1, S_2 and S_3 are exactly the same as for class 2 3. Thus when asking about the selection rules for the indexes, the reader has just to refer to Table V.

Turning to Table III, we observe that the major difference between class 2 3 and class 4 3 m arises from the vanishing of the double relations between the dissolution constants displayed in this table. As the double relations disappear for tensors of even rank, we get

$$A_{L,M} = B_{L,M} \quad (39)$$

in Equation 37. As a result we can show after some mathematical rearrangements that the series S_3 can be rewritten as sums of terms in the forms $(\cos\theta\sin\theta)^{2k}$ and $(\cos\theta)^{2m}(\sin\varphi\cos\varphi\cos^2\theta)^{2l}$. Then the dissolution constants which are included in the expressions for the coefficients $A_{L,M}$ and $B_{L,M}$ (i.e. for the coefficients $\mathscr{C}_{L,M}$) contribute now to the coefficients a_k and $b_{l,m}$. This remark is also valid for the complete expressions of coefficients $\mathscr{D}_{Q,R}$; the dissolution constants appearing in these expressions are now accounted for in the coefficients $d_{s,t}$. Denoting for convenience the transformed coefficients a_k^*, b_l^*, m and $d_{s,t}^*$ gives the following reduced expression for L

$$L = S_1^* + S_2^* + \mathscr{S}_1 + \mathscr{S}_2^* \quad (40)$$

where S_1^*, S_2^* and $\mathscr{S}_2^*$ are given by equations similar to the respective Equations 23, 24 and 29, except that the coefficients a_k, $b_{l,m}$ and $d_{s,t}$ are now replaced by the transformed coefficients. The selection rules as stated in Table V remain here again unchanged.

Finally, for the centrosymmetric classes 4 3 2 and m 3 m the series $\mathscr{S}_1$ and $\mathscr{S}_2^*$ involved in Equation 40 disappear and we obtain

$$L = S_1^* + S_2^* \quad (41)$$

We have just derived all the generalized expressions for the slowness surface of crystals belonging to the cubic system. These expressions must be used with the help of selection rules as well as with the requirements of symmetry conditions affecting the coefficients (Equations 30 to 35).

3. Theoretical results for class 2 3

Some attempts are made to correlate the more and less complicated shapes of various dissolution slowness surfaces to the appearance of certain crystal faces which limit the contour of etched crystals. For this purpose we have chosen firstly to deal with a hypothetical crystal belonging to class 2 3, and secondly to increase progressively the rank N_{max} in order to generate successive slowness surfaces which deviate more and more from the isotropic slowness surface.

3.1. The successive slowness surfaces for class 2 3

A spherical slowness surface is connected to an isotropic etching process. Examining Equations 22 to 29 it also readily appears that as the rank N_{max} remains smaller than three, only the radius $\mathscr{R}_0$ of the isotropic slowness surface can be affected by the value of N_{max}. But increasing the higher rank N_{max} from 3 to 10 gives rise to more and more complicated topologies. Here the coefficients a_k, $b_{l,m}$, $\mathscr{C}_{L,M}$, c_r, $d_{s,t}$ and $\mathscr{D}_{Q,R}$ have been modified with increasing N_{max} in such a way that

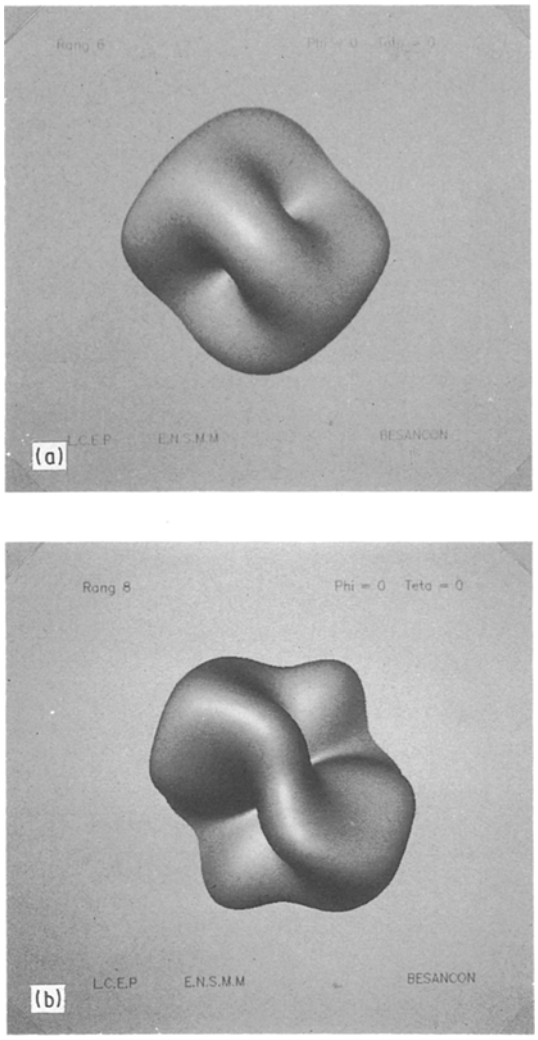

Figure 2 Slowness surfaces (a) Rang 6 (b) rang 8

the successive slowness surfaces remain crudely circumscribed in the initial sphere ($N_{max} = 0$).

A three-dimensional graphical representation of the slowness surface with N_{max} varying from 0 to 10 has been worked out on a SUN workstation (SUN 4/110) using the Phong style shading (50) with a palette of 256 colours. The workstation offers a high screen resolution, typically the display uses 1152×900 pixels. The results are displayed in Figs 1–3. In Figs 1–3a, the direction of observation $\mathbf{D}_{obs}$ which lies normal to the plane of figures is taken along the x_1 axis. As soon as N_{max} reaches 3, the general topology deviates from the isotropic sphere and is for certain directions pushed toward the spherical surface. Moreover, with increasing values of N_{max} the slowness surface seems to be more and more distorted and the geometries become so complicated that they cannot be described in detail. One may also observe that as N_{max} varies from 3 to 10, the slowness surface exhibits extrema corresponding to certain orientations; obviously the total number of extrema tends to increase with N_{max}. For $N_{max} = 10$, the slowness surface deviates considerably from a sphere. Then it may be of interest to change the direction $\mathbf{D}_{obs}$; for this reason in Fig. 3 the direction $\mathbf{D}_{obs}$ is successively taken along the directions [1 0 0],

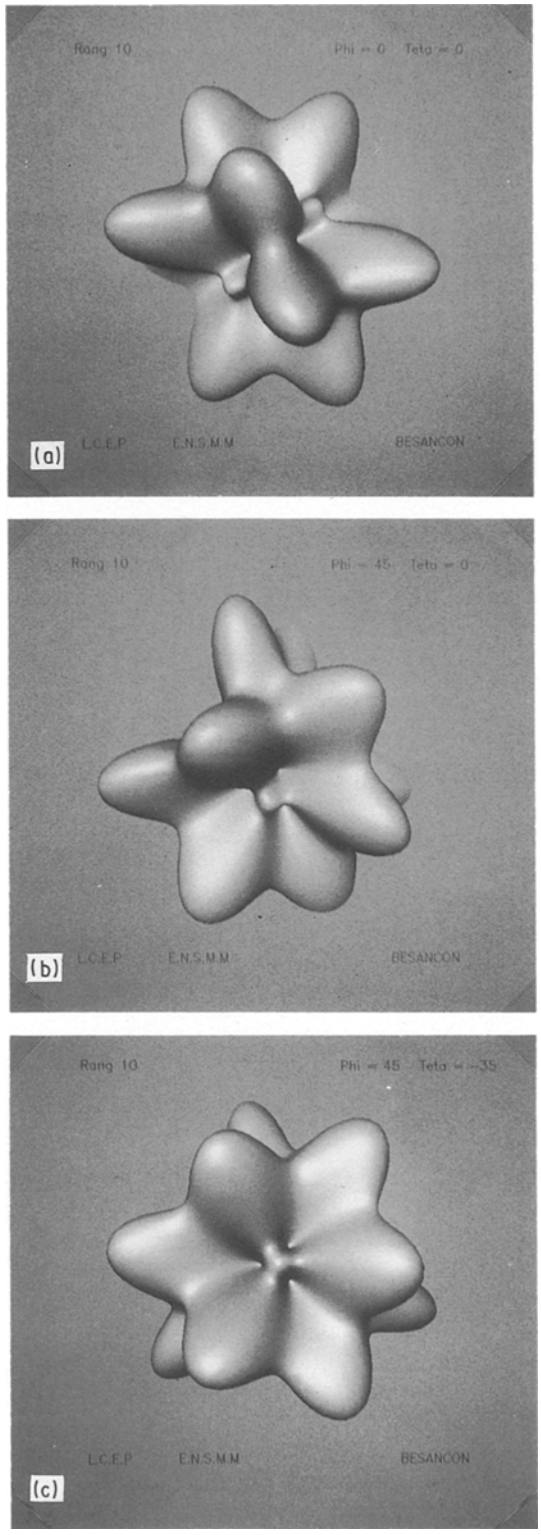

Figure 3 Slowness surfaces (a) [100]; (b) [110]; (c) [111]; rang = 10

[1 1 0] and [1 1 1]. To show more precisely how N_{max} affects the topology of the slowness surface, the shape of sections with fixed values of φ, i.e. $\varphi_0 = 0°$ and $\varphi_0 = 60°$ are displayed in Figs 4 and 5. It should be pointed out that we thus obtain polar graphs of **L** lying in the (1 0 0) plane and in a plane close to the $(\bar{2}\,1\,0)$ plane, respectively. As expected, we observe that increases in the value of N_{max} cause the formation of additional extrema in the polar plot of the dissolution slowness whose orientations correspond to some particular values, θ_e, of the angle of cut, θ. In reality the

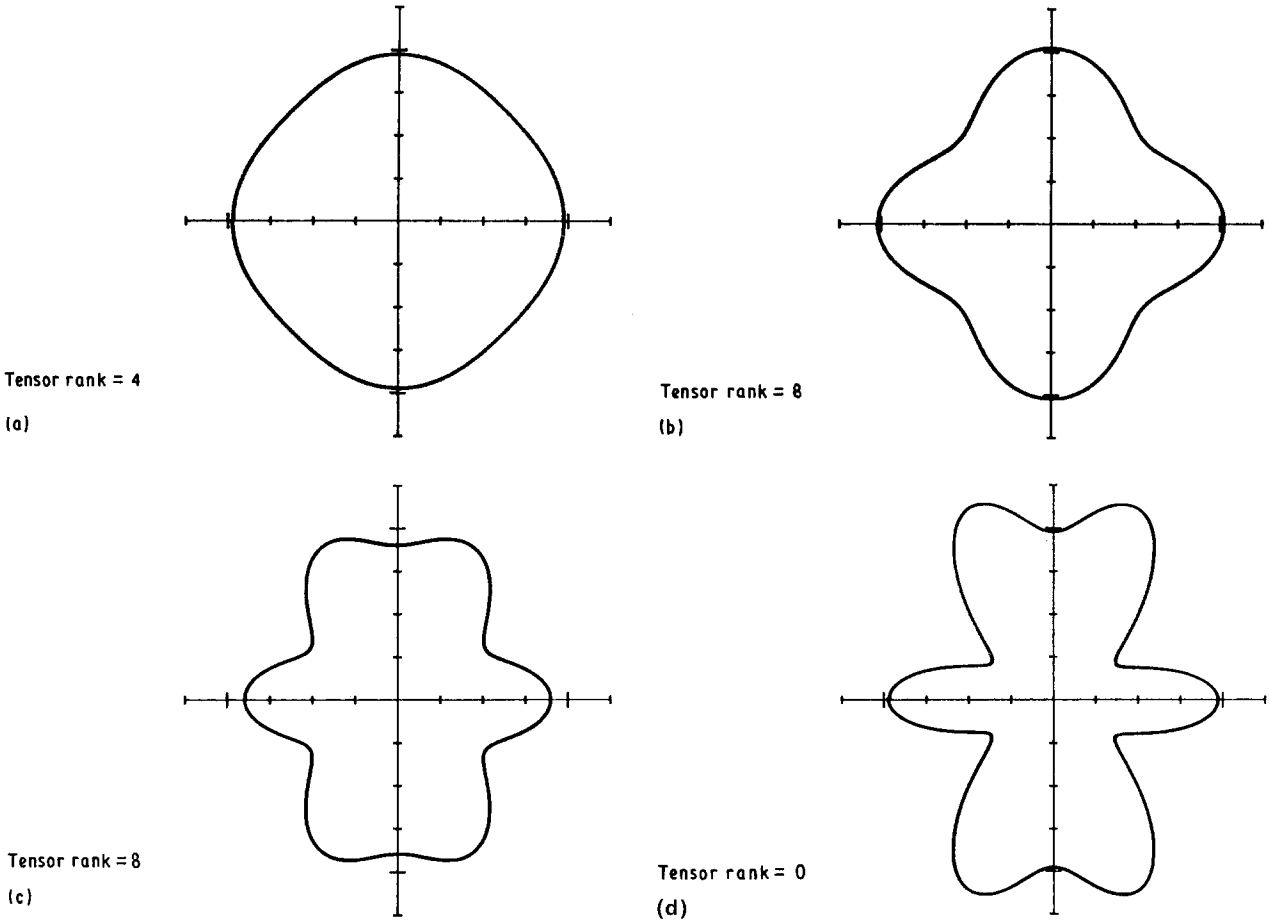

Figure 4 Slowness surface with $\varphi_0 = 0$

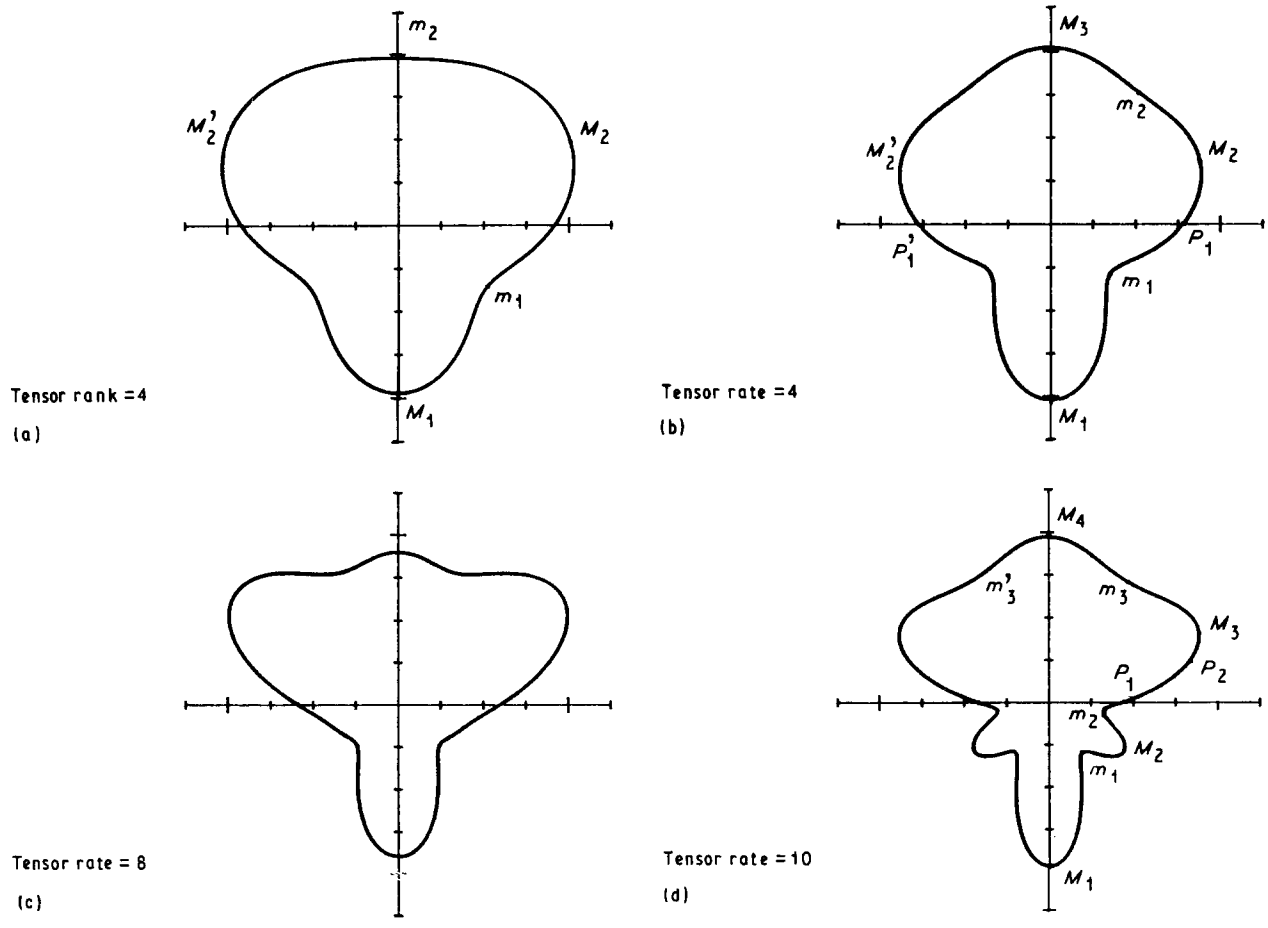

Figure 5 Slowness surface with $\varphi_0 = 60°$

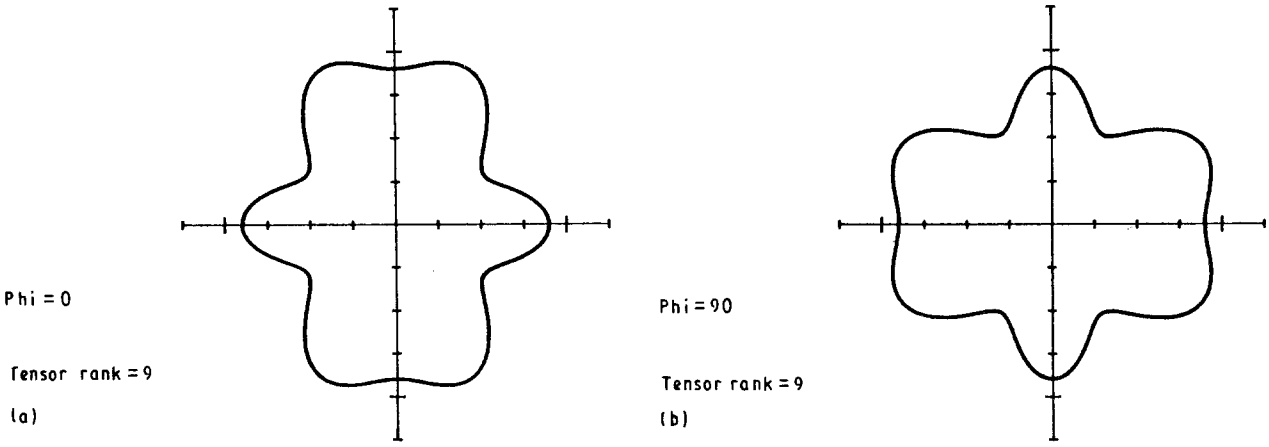

Figure 6 Slowness surface with tensor rank of 9 (a) $\varphi = 0°$ (b) $\varphi = 90°$

amplitude as well as the position of the extrema are modified by changes in the value of N_{max}.

At this point it is interesting to verify whether the derived shapes satisfy the crystal symmetry. Firstly let us consider the polar graphs obtained for $N_{max} = 9$, setting $\varphi = 0$ and $\varphi = 90°$ (Fig. 6). Obviously we are now concerned with the respective (1 0 0) and (0 1 0) sections of the slowness surface. We readily observe that the symmetry operations 2 associated with the crystallographic axes x_1, x_2 and x_3 are satisfied. Moreover, as we can also permute cyclically, the two-fold axes the shapes of the polar graphs in the (1 0 0) and (0 1 0) sections must be similar, except that we pass from one graph to the other by a rotation of 90° about the x_1 axis. Examination of Fig. 6 shows that this symmetry requirement is also fulfilled. We can also try to start from the general Equation 22 to demonstrate this symmetry property. Setting $\varphi = 0°$ and $\varphi = 90°$ into Equation 22 and for convenience limiting N_{max} to 7 we obtain

$$L_{x_2x_3}(\varphi = 0°, \theta) = a_0 + a_1(\cos\theta \sin\theta)^2 + (\mathscr{C}_{0,1} + \mathscr{C}_{1,0})\cos^2\theta + (\mathscr{C}_{0,2} + \mathscr{C}_{1,1} + \mathscr{C}_{2,0}) \times \cos^4\theta + (\mathscr{C}_{1,2} + \mathscr{C}_{2,1} + \mathscr{C}_{3,0} + \mathscr{C}_{0,3})\cos^6\theta \quad (42)$$

and

$$L_{x_1x_3}(\varphi = 90°, \theta) = a_0 + a_1(\cos\theta \sin\theta)^2 + \mathscr{C}_{0,1}\cos^2\theta + \mathscr{C}_{0,2}\cos^4\theta + \mathscr{C}_{0,3}\cos^6\theta \quad (43)$$

It is left as an exercise for the reader to show that changing θ into $\theta + 90°$ (i.e. $\cos\theta$ into $\sin\theta$) in Equation 36 and rearranging gives just the equation for the $L_{x_1x_3}$ polar graph.

Secondly, let us recall that the [1 1 1] direction which coincides with a diagonal of a cube is a three-fold rotation axis. Then viewing the slowness surface along this direction, the symmetry operation 3 must be verified. It is sufficient to examine Fig. 3c to observe a complete fulfilment of this condition. Thus we conclude that the derived equation adequately reflects the symmetry of class 2 3.

4. Conclusions

The tensorial representation of the anisotropic dissolution process has been used to derive analytical expressions for the dissolution slowness surfaces of crystals belonging to cubic classes. It is shown that a complete exploitation of the procedure needs complementary relations between the coefficients which reflect the symmetry of the corresponding point group. Class 2 3 has been treated as an example, and calculations have been performed for different values of the higher rank, N_{max}. It clearly appears that as N_{max} increases from zero to ten, the slowness surface exhibits a more and more complex shape. This evolving shape is characterized by an increasing number of extrema; behaviour which is conveniently illustrated by polar diagrams lying in differently oriented sections of the slowness surface. Moreover, three-dimensional representations of the slowness surface as viewed along various crystallographic directions reveal that the slowness surface satisfies all the symmetry operations specific to the point group. In these conditions, the equations derived in Part I will be used in Part II to develop numerical and graphical procedures for describing the equilibrium shapes of crystals.

References

1. K. SANGWAL, "Etching of Crystals" (North-Holland, Amsterdam, 1987).
2. K. E. PETERSEN, *Proc. IEEE* **70** (1982) 420.
3. D. B. LEE, *J. Appl. Phys.* **40** (1969) 4569.
4. K. E. BEAN, *IEEE Trans. Electron Devices* **ED-25** (1978) 1185.
5. J. W. FAUST, in "The Surface Chemistry of Metals and Semiconductors", edited by H. C. Gatos (Wiley, New York, 1960) p. 151.
6. P. J. HOLMES, *Acta Met.* **7** (1959) 283.
7. B. W. BATTERMAN, *J. Appl. Phys.* **28** (1957) 1236.
8. F. C. FRANK and M. B. IVES, *ibid.* **31** (1960) 1996.
9. Y. TARVI, Y. KOMIYA and Y. HARADA, *J. Electrochem. Soc.* **118** (1971) 118.
10. D. W. SHAW, *ibid.* **128** (1981) 874.
11. G. DELAPIERRE, *Sensors and Actuators* **17** (1989) 123.
12. F. E. HOLMES and C. A. T. SALAMA, *Solid-State Electron.* **17** (1974) 791.
13. I. STOEV, E. SIMOV, E. SIMOVA, N. BONNET and G. BALOSSIER, *Sensors and Actuators* **12** (1987) 1.
14. S. K. CLARK and K. D. WISE, *IEEE Trans. Electron Devices*, **ED-26** (1979) 1887.
15. M. BAO and Y. WANG, *Sensors and Actuators* **12** (1987) 49.

16. K. E. PETERSEN, *IEEE Trans. Electron Devices* **ED-25** (1978) 1241.
17. R. J. WILFINGER, P. H. BARDELL and D. S. CHABRA, *IBM J. Res. Devel.* **12** (1968) 113.
18. G. KAMINSKY, *J. Vac. Sci. Tech.* **B3** (1985) 1015.
19. A. I. STOLLER, *RCA Rev.* June (1970) 271.
20. R. A. BUSER and N. F. DE ROOIJ, *Sensors and Actuators* **17** (1989) 145.
21. Y. LINDEN, L. TENERZ, J. TIREN and B. HOK, *ibid.* **16** (1989) 67.
22. K. YAMADA, M. NISHIHARA and R. KANZAWA, R. KOBAYASHI, *ibid.* **4** (1983) 63.
23. G. BLASQUEZ, P. PONS and A. BOUKABACHE, *ibid.* **17** (1989) 387.
24. W. H. KO, J. HYNECEK, S. F. BOETTCHER, *IEEE Trans. Electron Devices* **ED 26** (1979) 1896.
25. H. SEIDEL and L. CSEPREGI, *Sensors and Actuators* **4** (1983) 455.
26. P. M. SARRO and A. W. VAN HERWAARDEN, *J. Electrochem. Soc.* **133** (1986) 1724.
27. V. LINDEN, L. TENERZ, J. TIREN and B. HOK, *Sensors and Actuators* **16** (1989) 67.
28. O. J. GLEMBOCKI and R. E. STAHLBUSH, *J. Electrochem. Soc.* **132** (1985) 145.
29. M. J. DECLERCQ, L. GERZBERG and J. M. MEINDL, *ibid.* **122** (1975) 545.
30. M. M. ABU-ZEID, *ibid.* **131** (1984) 2138.
31. X-P WU and W. H. KO, *Sensors and Actuators* **18** (1989) 207.
32. Y. KANDA and A. YASUKAWA, *ibid.* **2** (1982) 283.
33. Y. KANDA, *ibid.* **4** (1983) 199.
34. M. BAO, W. QI and Y. WANG, *ibid.* **18** (1989) 149.
35. Y. KANDA and K. YAMAMURA, *ibid.* **18** (1989) 247.
36. SAMAUN, K. D. WISE and J. B. ANGELL, *IEEE Trans. BioMed. Engng* **20** (1973) 101.
37. W. G. PFANN and R. N. THURSTON, *J. Appl. Phys.* **32** (1961) 2008.
38. Y. WANG, M. BAO and L. YU, *Sensors and Actuators* **18** (1989) 221.
39. C. R. TELLIER and J. L. VATERKOWSKI, *J. Mater. Sci.* **24** (1989) 1077.
40. C. R. TELLIER and T. G. LEBLOIS, in Proceedings of the Third European Time and Frequency Forum, Besançon, France, 1989 (Imprimerie Conseil General du Doubs) pp. 246–255.
41. C. R. TELLIER, *J. Cryst. Growth* **100** (1990) 515.
42. C. R. TELLIER, T. G. LEBLOIS and P. C. MAITRE, *J. Mater. Sci.* **24** (1989) 3029.
43. C. R. TELLIER, *J. Cryst. Growth* **96** (1989) 450.
44. R. B. HEIMANN, in "Silicon Chemical Etching", edited by J. Grabmaier (Springer, Berlin, 1982) p. 197.
45. M. LIGHTHILL and G. WHITMAN, *Proc. Roy. Soc.* **A229** (1955) 281.
46. F. C. FRANK, in "Growth and Perfection of Crystals", edited by R. H. Doremus, B. W. Robert and D. Turnbull (Wiley, New York, 1985) p. 411.
47. C. R. TELLIER, N. VIALLE and J. L. VATERKOWSKI, *Surf. Coat. Technol.* **34** (1988) 417.
48. "Standard on Piezoelectricity" (IEEE, New York, 1978) p. 15.
49. J. F. NYE, "Propriétés Physiques des Cristaux" (Dunod, Paris, 1961).
50. D. F. ROGERS, "Procedural Elements for Computer Graphics" (MacGraw-Hill, New York, 1985).
51. C. R. TELLIER, J. Y. AMAUDRUT, A. BRAHIM BOUNAB, *J. Mater. Sci.* **26** (1991) 5595.

Received 18 June
and accepted 19 October 1990